

See discussions, stats, and author profiles for this publication at: <https://www.researchgate.net/publication/216796392>

# Measurement and Prediction of Interfacial Tension of Binary Mixtures

ARTICLE in INDUSTRIAL & ENGINEERING CHEMISTRY RESEARCH · DECEMBER 2009

Impact Factor: 2.59 · DOI: 10.1021/ie901209z

CITATIONS

22

READS

68

## 4 AUTHORS:



**Gabriel Nino-Amezquita**

Technische Universität Berlin

4 PUBLICATIONS 59 CITATIONS

SEE PROFILE



**Sabine Enders**

Technische Universität Berlin

47 PUBLICATIONS 475 CITATIONS

SEE PROFILE



**Philip T. Jaeger**

Eurotechnica

43 PUBLICATIONS 370 CITATIONS

SEE PROFILE



**Rudolf Eggers**

Technische Universität Hamburg-Harburg

78 PUBLICATIONS 834 CITATIONS

SEE PROFILE

# Measurement and Prediction of Interfacial Tension of Binary Mixtures

Oscar G. Nino-Amezquita,<sup>†</sup> Sabine Enders,<sup>\*,†</sup> Philip T. Jaeger,<sup>‡</sup> and Rudolf Eggers<sup>‡</sup>

*Institute of Process Engineering, Department of Thermodynamics and Thermal Engineering, TU Berlin, TK7, Straße des 17. Juni, 10623 Berlin, Germany, and Department of Thermal Separation, Processes, Heat and Mass Transfer, TU Hamburg - Harburg, Eißendorfer Strasse 38, 21073 Hamburg, Germany*

The density gradient theory was combined with a modern equation of state based on statistical mechanics, the perturbed chain-statistical association fluid theory, or with the well-known Peng–Robinson equation of state, and is applied to compute the surface tension of various binary mixtures made up of nonpolar substances. Additionally, some new data for the system methane + hexane and methane + heptane were measured using the pendant drop method equipped with a high-pressure cell. Both equations of state can be used to predict the surface tension of mixtures very close to experimental data. The surface tension of pure ethane could also be predicted using the surface tension data of other *n*-alkanes. Additionally, the surface tensions for mixtures as a function of liquid composition, of temperature, and of pressure were calculated for systems, where no experimental data are available. If the mixture contains a high volatile component, strong relative enrichment effects in the interface could be observed.

## Introduction

The importance of reliable determination of interfacial tension between fluid phases has been well recognized in the oil industry, especially in the enhanced oil recovery process. With an increased number of gas condensate fields being discovered worldwide as exploration drilling of greater depth encounters high-pressure and high-temperature conditions, the determination of low or ultralow gas condensate interfacial tensions becomes important. For example, the product of the surface tension and the cosine of the contact angle between reservoir rock and brine is one of the determining factors for the gas, which can be recovered. Because the surface tension is directly proportional to the capillary pressure, the variation of surface tension with temperature and pressure strongly influences the transport of the media in a reservoir.

Interfacial properties of solvent mixtures at conditions closed to the boiling point of these mixtures are also important for technical polymerization process because mostly the solution polymerization process is performed close to these conditions to handle the polymerization heat in an optimal way. Additionally, interfacial properties between fluid phases play an important role in technical separation processes like distillation, absorption, and extraction.

Because of the cost of the experiments involved and the scarcity of data, a theoretical approach to provide surface tension information without performing experiments will be very valuable. This statement holds true, in particularly if high volatile components such as light *n*-alkanes are present in the mixture. Caused by the high vapor pressure of these substances, it is impossible to measure the surface tension of these systems at different compositions and at different temperatures using the standard methods, like ring or plate method. Only experiments using a closed system, like the pendant drop method equipped with a high-pressure cell, are possible.

In this Article, the density gradient theory (DGT), developed by Cahn and Hilliard<sup>1</sup> as well as Poser and Sanchez,<sup>2</sup> is applied for modeling the interfacial properties of planar interfaces in

binary systems between two fluid phases. The DGT of inhomogeneous systems provides a means for relating an equation of state to interface properties and leads to a general expression for the Helmholtz free energy density of an inhomogeneous system. Using this expression in combination with an equation of state (or Peng–Robinson equation of state<sup>3–6</sup>), a method was developed for calculating the surface tension and density profiles of mixtures in equilibrium with its vapor. The most important prerequisite for the successful application of the theoretical framework is the accurate description of the vapor–liquid equilibrium (VLE) of the considered mixture.

Modern equations of state based on statistical mechanics are able to model the phase equilibrium of mixtures in satisfactory agreement with experimental findings. One family of this type of equation is the so-called SAFT (statistical association fluid theory) family. A review of the application of different versions within this family is given by Müller and Gubbins.<sup>7</sup> The application of SAFT-EOS to mixtures made from molecules that are of interest in this Article has been proven in several papers.<sup>8–12</sup> This equation of state was successfully combined with the DGT to calculate the surface tension of pure components<sup>13</sup> and binary mixtures.<sup>14,15</sup>

Gross and Sadowski<sup>16,17</sup> as well as Chapman et al.<sup>18–20</sup> developed the PC-SAFT (perturbed chain-statistical association fluid theory) by applying the perturbation theory of Barker and Henderson<sup>21</sup> to a hard-chain reference fluid. This version of the SAFT family was used to calculate phase equilibria of different mixtures, including solvent of different kinds, polymers, and copolymers. In this Article, PC-SAFT is used for the first time as equation of state in the DGT framework, because the DGT permits one to calculate the surface tension as well as other interfacial properties, like interfacial density profiles, interfacial thickness, and relative enrichment of one component in the interface only from the EOS, where the parameter can be adjusted to bulk properties, and one surface tension at one temperature of the pure component. For this reason, the interfacial properties of mixtures are really predictions.

In the last 15 years, the DGT has developed to a widely used method for the calculation of interfacial properties.<sup>22–26</sup> Another theoretical framework, similar to the DGT, is the application

\* To whom correspondence should be addressed. E-mail: sabine.enders@tu-berlin.de.

<sup>†</sup> TU Berlin.

<sup>‡</sup> TU Hamburg - Harburg.

of the density functional theory in combination with an equation of state.<sup>27–29</sup>

The goal of this study is to incorporate the PC-SAFT-EOS in the DGT, to compare the results with calculations carried out with the PR-EOS, and to evaluate the extent to which the DGT is applicable to predict the surface tensions of mixtures as a function of temperature, pressure, and composition. To evaluate the performance of the theory, we have performed some measurements, especially in case no data were available in the literature.

## Experiments

Among a great number of methods to measure interfacial tension, the pendant drop technique, which was introduced by Andreas et al.,<sup>30</sup> has proved to be one of the most practicable methods for systems under high pressure. For determination of the interfacial tension from the profile of a pendant drop, the Laplace equation,<sup>31</sup> which is based on equilibrium of forces, is used. The experiments were carried out using the high-pressure pendant drop equipment PD-E1700, Eurotechnica GmbH.<sup>32</sup> The equipment can be applied at pressures up to 70 MPa and up to 200 °C. The pressure was determined by a pressure transducer (WIKA, 1–100 MPa) at an accuracy of  $\pm 0.01$  MPa. The temperature was measured by a thermocouple within the view chamber to an accuracy of  $\pm 0.1$  °C. The drop profiles were recorded at different drop ages to determine the thermodynamic equilibrium. Drop ages between 10 and 60 min were achieved. Measurements were repeated usually evaluating at least three different drops. The interfacial tension data were determined at an accuracy of  $\pm 0.3$  mN/m. For evaluating the experimental drop profiles, the drop images were recorded by a CCD camera connected to a personal computer with an automatic image processing. The software program “Drop Shape Analysis” (Kruss, Germany) evaluates the drop shape to solve the differential equations numerically. To solve the differential equations, the robust shape method, which proved to be stable toward runaways, that may occur due to insufficiencies of the image processing, is employed.<sup>32–36</sup>

For calculating the interfacial tension from the recorded drop profiles, the density difference between the liquid and the dense gas must be known. Experimental and theoretical literature data<sup>37</sup> were used to determine the temperature- and pressure-dependent densities of the contacting hydrocarbon phases. Heptane and hexane were supplied by ACROS at a purity of 99.9%. Methane was obtained from Westfalen Gas at a purity of 99.999%.

**Theoretical Approach.** Before any surface properties can be computed, it is necessary to find the thermodynamic equilibrium densities between which the interface is formed. The densities of the vapor and the liquid phase can be calculated at a given temperature and pressure. Such calculations are carried out by equating the chemical potentials and the pressures in both coexisting phases. For practical applications, the choice of an equation of state depends on the computing time involved, accuracy, and theoretical soundness.

In the past, the cubic EOS has been especially popular because of their simplicity and their applicability to a wide range of systems, if no substance with special interactions, like dipolar or association interaction, is present in the mixture. One equation of this family is the famous Peng–Robinson equation of state (PR-EOS).<sup>38</sup> The properties of the mixtures of nonpolar fluids are estimated by the PR-EOS, which is expressed as:

$$P = \frac{RT}{V-b} - \frac{a(T)}{(V^2 + 2Vb - b^2)} \quad (1)$$

The PR-EOS was chosen because of its widespread use in industry and its simplicity. The parameters  $a$  and  $b$  were calculated from the critical data,  $T_C$  and  $P_C$ , and the acentric factor,  $w$ , according to:

$$b = \frac{0.0778RT_C}{P_C}$$

$$a = \frac{0.45724R^2T_C^2}{P_C} \left[ 1 + (1 + 0.37464 + 1.54226\omega - 0.26992\omega^2) \left( 1 - \sqrt{\frac{T}{T_C}} \right) \right]^2 \quad (2)$$

The parameters  $a$  and  $b$  for binary mixtures were obtained using the van der Waals mixing rules:

$$a = \sum_i \sum_j X_i X_j a_{ij} \quad a_{ij} = (1 - k_{ij}) \sqrt{a_i a_j} \quad b = \sum_i X_i b_i \quad (3)$$

Using standard thermodynamic values, equations for the Helmholtz energy and for the chemical potentials of both components can be derived. For example, the chemical potential for the component  $i$  using eq 1 is given by:

$$\frac{\mu_i - \mu_i^{\text{ideal}}(P)}{RT} = \ln\left(\frac{V}{V-b}\right) + \frac{b_i}{V-b} - \ln\left(\frac{PV}{RT}\right) - \frac{1}{RTb\sqrt{2}} \left( \frac{ab_i}{2b} - (x_i a_i + (1-x_i)\sqrt{a_i a_j}(1-k_{ij})) \right) \times \ln\left(\frac{V+b(1-\sqrt{2})}{V+b(1+\sqrt{2})}\right) - \frac{ab_i V}{RTb(V^2 + 2bV - b^2)} \quad (4)$$

The PC-SAFT-EOS can be expressed via different contributions to the Helmholtz energy:<sup>16,17</sup>

$$\frac{F}{RT} = \frac{F^{\text{ideal}}}{RT} + \frac{F^{\text{chain}}}{RT} + \frac{F^{\text{disp}}}{RT} + \frac{F^{\text{asso}}}{RT} \quad (5)$$

The first term in eq 5 describes the mixture of ideal gases. The term  $F^{\text{chain}}$  is the hard-chain reference contribution, where the chain is formed from hard spheres. According to the perturbation theory of Barker and Henderson,<sup>21</sup> the attractive part of the chain interactions ( $F^{\text{disp}}$  in eq 5) is given as a sum of first- and second-order contributions. The last term in eq 5 takes the association into account. This term is not used here, because we consider only molecules without association interaction. For nonassociating molecules, three pure-component parameters, the segment diameter  $\sigma$ , the depth of pair potential  $\epsilon$ , and the number of segments per chain  $m$ , enter the PC-SAFT-EOS. Usually the pure-component parameters were fitted to the vapor pressure and the liquid volume. More details can be found elsewhere.<sup>16,17</sup>

The Cahn–Hilliard Theory<sup>1</sup> describes the thermodynamic properties of a system where an interface exists between two fluid phases. At thermodynamic equilibrium, the pressure, the temperature, and the composition in the bulk phases are fixed by the thermodynamics equilibrium conditions. For pure components, only the density changes within the interface. For binary mixtures, the density as well as the concentration will change throughout the interface. To take both effects into account, we define the partial densities  $\rho_i$ .

$$\rho_i = X_i \rho \quad (6)$$

where  $X_i$  is the mole fraction of component  $i$ , and  $\rho$  is the density of the mixture.

Usually, the thermodynamic quantities of binary systems made from the components A and B at constant temperature are functions of density and composition, expressed by mole fraction (e.g., Helmholtz energy  $F(\rho, X_i)$ ). Applying eq 1 or 5, the thermodynamic functions can be rewritten as functions of both partial densities (e.g.,  $F(\rho_A, \rho_B)$ ). Using a similar procedure, like Cahn and Hillard,<sup>1</sup> to calculate the interfacial tension of a planar interface, Poser and Sanchez<sup>2</sup> worked out a method that considers the change of two variables ( $\rho_A, \rho_B$ ) within the interface. The interfacial tension between two fluid phases in equilibrium reads:

$$\begin{aligned}\sigma &= 2^{1/2} \int_{\rho_B^I}^{\rho_B^H} \left[ \kappa_B + 2\kappa_{AB} \left( \frac{d\rho_A}{d\rho_B} \right) + \kappa_A \left( \frac{d\rho_A}{d\rho_B} \right)^2 \right]^{1/2} \Delta\omega^{1/2} d\rho_B \\ &= 2^{1/2} \int_{\rho_B^I}^{\rho_B^H} \sqrt{\kappa' \Delta\omega} d\rho_B\end{aligned}\quad (7)$$

where  $\kappa'$  results from the so-called influence parameters of the pure components,  $\kappa_i$ , and  $\Delta\omega$  is the grand thermodynamic potential. The limits of integration  $\rho_B^I$  and  $\rho_B^H$  are the partial densities in the coexisting phases and can be obtained by eq 1 or 5. The grand thermodynamic potential  $\Delta\omega$  for binary mixtures results in:

$$\begin{aligned}\Delta\omega &= (F(T, V, X_B) - X_A\mu_A^V - X_B\mu_B^V + PV)\rho \\ &= \rho_A(\mu_A - \mu_A^V) + \rho_B(\mu_B - \mu_B^V)\end{aligned}\quad (8)$$

The Helmholtz energy,  $F$ , and the chemical potentials,  $\mu_i$ , can be obtained by an equation of state, if the quantities  $\rho_A$  and  $\rho_B$  are known. Therefore, the calculation of  $\Delta\omega$  needs the knowledge of  $\rho_A$  for each value of  $\rho_B$  within the interface. This dependence is in agreement with the density profiles through the interface.

The  $\kappa_i$ -parameter with  $i = A$  or  $B$  in eq 7 can be adjusted to one experimental surface tension of the pure component at one temperature. The parameter  $\kappa_{AB}$  can be calculated using the geometrical average of the pure-component parameters:

$$\kappa_{AB} = \sqrt{\kappa_A \kappa_B} \quad (9)$$

This situation allows the prediction of the surface tension of binary mixtures as a function of temperature, pressure, and composition because only information about the bulk phase via the EOS and one surface tension of pure components, which can be found in a database,<sup>39</sup> enter the theoretical framework.

During derivation of eq 7, transformation of the coordinates from the local space to the density space was used.<sup>2</sup> The integration of this transformation permits the calculation of the density profiles with the following expression:

$$z = z_0 + \int_{\rho_B(z_0)}^{\rho_B(z)} \sqrt{\frac{\kappa'}{\Delta\omega}} d\rho_B \quad (10)$$

where  $\kappa'$  is given in eqs 7 and 9, and  $z_0$  represents an arbitrarily chosen origin. The symmetrical interface segregation within the interface,  $\Delta C(z)$ , is applied for the qualitative analysis of the density profiles. Following da Gama and Evans<sup>40</sup> as well as Winkelmann and Wadewitz,<sup>41</sup> it is given by:

$$\begin{aligned}\Delta C(z) &= \frac{\rho_A(z) - \rho_A^L}{a_A} - \frac{\rho_B(z) - \rho_B^L}{a_B} a_i \\ &= \frac{\rho_i^L - \rho_i^V}{\rho_A^L - \rho_A^V + \rho_B^L - \rho_B^V}\end{aligned}\quad (11)$$

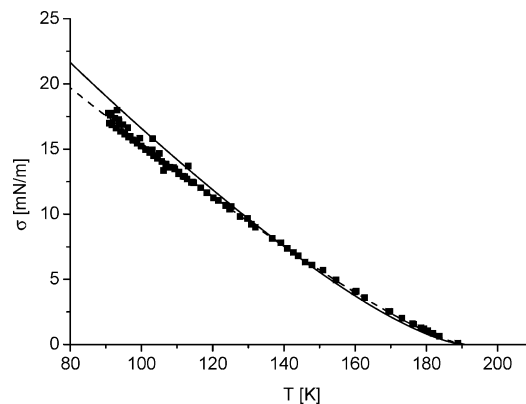


**Figure 1.** Comparison of experimental<sup>39</sup> (symbols) and calculated surface tensions of methane using PR-EOS (solid line) or PC-SAFT-EOS (broken line).

The symmetrical interface segregation,  $\Delta C(z)$ , leads directly to an expression for the relative adsorption  $\Gamma_{BA}$  within the interface.<sup>40,41</sup>

$$\Gamma_{BA} = -a_B \int_{-\infty}^{+\infty} \Delta C(z) dz \quad (12)$$

Another important quantity, which can be derived from the density profiles, is the thickness of the interface. This thickness is thermodynamically not exactly defined. To specify a physical value, the 10/90-rule, given by Lekner and Henderson,<sup>42</sup> was used.

## Results

To predict the surface tension of the mixture, the influence parameter of the pure components must be known. For this reason, first the calculation of surface tension of pure components is discussed. Second, systems containing methane and different  $n$ -alkanes having carbon numbers from five until seven will be considered. The next type of mixture consists of cyclohexane + different  $n$ -alkanes having carbon numbers from three to seven. Finally, the application of the theoretical framework is checked also for aromatic substances by investigating the system heptane + toluene.

**1. Pure Substances.** Using the PR-EOS, the pure-component parameters were estimated using critical data and acentric factors.<sup>45</sup> The pure-component parameters in combination with PC-SAFT-EOS were taken from the literature.<sup>16</sup> During the fitting procedure, vapor–pressure data and liquid volumes were used.<sup>16</sup> Both equations of state are able to model the phase diagram of  $n$ -alkanes very close to the experimental data.

The critical point of methane ( $T_C = 190.56$  K and  $P_C = 4.595$  MPa) is located at very low temperatures. The surface tension can only be measured at these low temperatures. Therefore, if the surface tension of mixtures containing methane at room temperatures should be calculated, an extrapolation of the influence parameter of methane from temperatures below the critical point to room temperatures must be done. Figure 1 shows the experimental surface tensions as a function of temperature, taken from the literature,<sup>39</sup> in comparison with calculated surface tensions using PR-EOS or PC-SAFT-EOS. The influence parameters were estimated at one temperature, close to 140 K. First, both equations of state are able to calculate the surface tension of methane very close to the experimental values. At very low temperatures (below 120 K), the surface tension calculated with the PR-EOS is slightly higher than the surface tension calculated with the PC-SAFT-EOS. The estimated influence parameter is listed in Table 1.



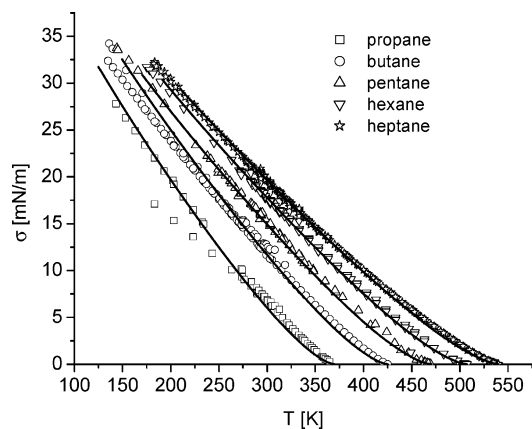
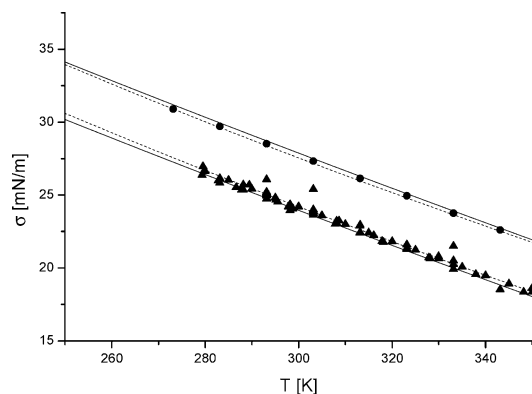
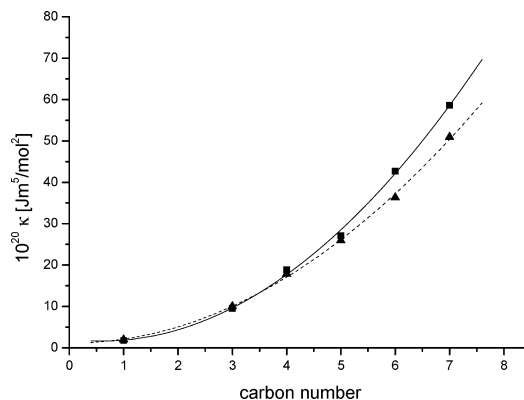
**Table 1. Estimated Influence Parameters,  $\kappa_i$ , for the Pure Components Using Eq 1 or 5**

| pure component | $10^{20} \kappa$ [ $\text{J} \cdot \text{m}^5/\text{mol}^2$ ] | $10^{20} \kappa$ [ $\text{J} \cdot \text{m}^5/\text{mol}^2$ ] |
|----------------|---|---|
|                | PR-EOS  | PC-SAFT-EOS   |
| methane        | 1.764   | 1.973   |
| propane        | 9.547   | 10.00   |
| butane         | 18.826  | 17.81   |
| pentane        | 27.1  | 25.91   |
| hexane         | 42.67   | 36.298  |
| heptane        | 58.6  | 50.92   |
| toluene        | 37.162  | 31.89   |
| cyclohexane    | 32.518  | 34.07   |

In Figure 2, the calculated surface tensions of *n*-alkanes with carbon numbers from three to seven using PR-EOS or PC-SAFT-EOS are plotted as a function of temperature. Additionally, the experimental values, taken from the literature,<sup>39</sup> are also given in this figure. From this figure, it can be concluded that both equations of state are able to model the surface tension. In this figure, no significant difference between both equations can be recognized. The estimated influence parameters are also given in Table 1.

In Figure 3, the calculated surface tensions of cyclohexane and toluene using both equations are compared to the experimental data, taken from the literature.<sup>39</sup> Again, both equations are able to model the surface tension in excellent agreement with experimental data. The estimated influence parameters are also given in Table 1.

Using the estimated  $\kappa$ -parameters from Table 1 in combination with the PR-EOS or PC-SAFT-EOS, the surface tension

**Figure 2.** Comparison of experimental<sup>39</sup> (symbols) and calculated surface tensions using PR-EOS (solid line) or PC-SAFT (broken line) of pure *n*-alkanes.**Figure 3.** Comparison of experimental (cyclohexane  $\blacktriangle$ ,<sup>39</sup> toluene  $\bullet$ )<sup>39</sup> and calculated surface tensions of pure components using PR-EOS (solid line) or PC-SAFT (broken line).**Figure 4.** Estimated influence parameters,  $\kappa_i$ , for alkanes as a function of carbon number using PR-EOS ( $\blacksquare$ ) or PC-SAFT ( $\blacktriangle$ ). The lines are fitted to the corresponding  $k$ -values.

of the pure components can be modeled over a broad temperature range in excellent agreement with experimental data taken from the literature.<sup>39</sup> A test of plausibility for the physical background of the selected model is the dependence of the influence parameter from the number of carbon atoms. In Figure 4, the  $\kappa_i$ -values of Table 1 are plotted as a function of the carbon number. It can be seen that the  $\kappa_i$ -parameter increases continuously with the carbon number.

The data given in Table 1 or in Figure 4 can be used to fit a polynomial expression for  $\kappa$  as a function of the carbon number  $N$ . The fitting using PR-EOS results in:

$$\kappa_{\text{alkanes}}^{\text{PR-EOS}} = (2.10927 - 1.64958N + 1.3878N^2)10^{-20} \frac{\text{J} \cdot \text{m}^5}{\text{mol}^2} \quad (13)$$

The polynomial expression for the  $\kappa$ -values using PC-SAFT-EOS is:

$$\kappa_{\text{alkanes}}^{\text{PC-SAFT}} = (1.17164 - 0.09767N + 1.0178N^2)10^{-20} \frac{\text{J} \cdot \text{m}^5}{\text{mol}^2} \quad (14)$$

Ethane was not included in the parameter estimation. Using eq 13 or eq 14, the  $k$ -value for ethane can be calculated, and the surface tension of ethane as a function of temperature can be predicted. Using eq 13 with  $N = 2$  results in  $\kappa_{\text{ethane}} = 4.3613 \times 10^{-20} \text{ J} \cdot \text{m}^5/\text{mol}^2$ , and using eq 14 with  $N = 2$  the  $\kappa$ -value should be  $\kappa_{\text{ethane}} = 5.0475 \times 10^{-20} \text{ J} \cdot \text{m}^5/\text{mol}^2$ . The predicted surface tensions together with experimental values taken from the literature<sup>39</sup> are depicted in Figure 5. Again, both models do an excellent job in surface tension calculation of ethane.

In summary, both models are able to calculate the surface tension as a function of temperature for *n*-alkanes and other nonpolar substances, like cyclohexane and toluene.

**2. Mixtures Containing Methane + *n*-Alkane.** The next step for the prediction of surface tensions of mixtures is the calculation of the corresponding phase diagrams. These calculations can be applied to estimate the binary interaction parameter  $k_{ij}$ . Figure 6 shows the vapor–liquid phase behavior for the system methane + heptane at different temperatures. Using one temperature-independent  $k_{ij} = 0.03$  for both equations of state, the phase equilibria can be modeled in satisfactory agreement with experimental data, taken from the literature.<sup>43</sup> The  $k_{ij}$ -value was fitted to the isobaric phase diagram at  $P = 0.101 \text{ MPa}$ . For this reason, some problems arise for both equations in the region of high pressures.

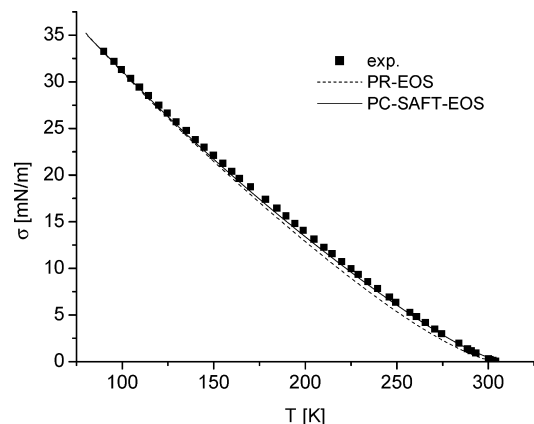


**Figure 5.** Experimental<sup>39</sup> and predicted surface tension for ethane using PR-EOS with eq 13 or PC-SAFT-EOS with eq 14.

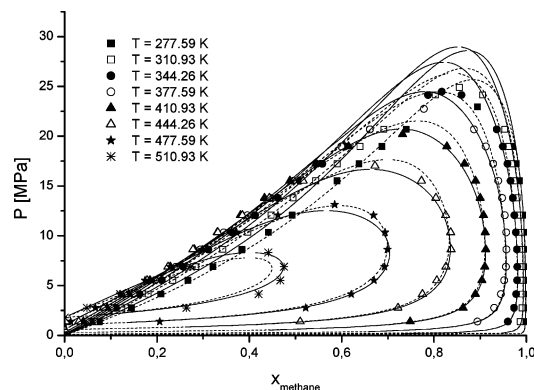


**Figure 6.** Experimental<sup>43</sup> and calculated phase compositions for the system methane + heptane using PC-SAFT-EOS (solid line) or PR-EOS (broken line) with  $k_{ij} = 0.03$ .

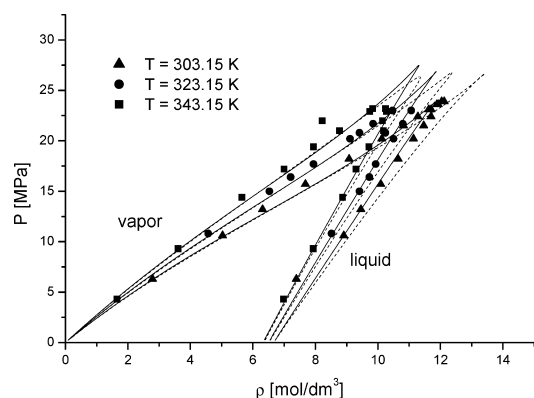


**Figure 7.** Experimental<sup>44</sup> and calculated densities in the coexisting phases (vapor and liquid) using PC-SAFT-EOS (solid line) or PR-EOS (broken line) with  $k_{ij} = 0.03$  for the system methane + heptane.

Besides the phase composition, the phase densities, especially in the liquid phase, are very important for the surface tension calculations. In Figure 7, the calculated and experimental<sup>44</sup> densities of the coexisting phases at three different temperatures are demonstrated. Similar to the calculations of the phase composition, the calculated densities agree very well with experimental data, but some derivation occurs in the high-pressure range. This finding can be very important, because during pendant drop experiments the density of the coexisting phases must be known. Usually, the measurements of the densities of mixtures at high pressure are very time-consuming. Using a suitable equation of state this type of measurement can

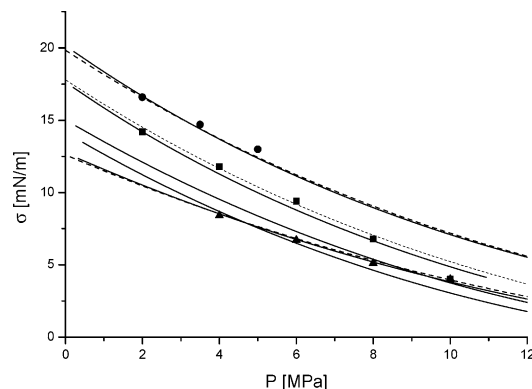


**Figure 8.** Comparison between the measured (● hexane at  $T = 298.15$  K, ▲ hexane at  $T = 350.15$  K, and ■ heptane  $T = 298.15$  K) and predicted surface tensions using PC-SAFT-EOS (solid line for pentane and hexane with  $k_{ij} = 0$  and for heptane  $k_{ij} = 0.03$ ) or PR-EOS (broken line pentane and hexane with  $k_{ij} = 0$  and for heptane  $k_{ij} = 0.03$ ) for different alkanes in methane atmosphere.

**Table 2.** Experimental Data

| <i>n</i> -alkane  | <i>T</i> [K] | <i>P</i> [MPa] | $\sigma$ [mN/m] |
|-------------------|--------------|----------------|-----------------|
| <i>n</i> -hexane  | 300          | 2              | 14.2            |
| <i>n</i> -hexane  | 300          | 4              | 11.8            |
| <i>n</i> -hexane  | 300          | 6              | 9.4             |
| <i>n</i> -hexane  | 300          | 8              | 6.8             |
| <i>n</i> -hexane  | 300          | 10             | 4               |
| <i>n</i> -hexane  | 350          | 4              | 8.4             |
| <i>n</i> -hexane  | 350          | 6              | 6.7             |
| <i>n</i> -hexane  | 350          | 8              | 5.1             |
| <i>n</i> -hexane  | 350          | 10             | 4               |
| <i>n</i> -heptane | 298.15       | 2              | 16.6            |
| <i>n</i> -heptane | 298.15       | 3.5            | 14.7            |
| <i>n</i> -heptane | 298.15       | 5              | 13              |

be reduced to a minimum. The measurements are only necessary to verify the quality of the selected equation of state.

Using the  $\kappa$ -parameters given in Table 1, the mixing rule for  $\kappa$  (eq 9) and the binary interaction parameter,  $k_{ij}$ , fitted to the bulk phase behavior, the surface tension of mixtures can be predicted. The phase equilibria for the system methane + pentane and for the system methane + hexane can be calculated using  $k_{ij} = 0$ , independent from the equation of state to be used. Figure 8 depicts the predicted surface tension of mixtures containing methane + *n*-alkane with carbon numbers from five to seven. The experimental data for the systems methane + hexane and methane + heptane given in Figure 8 and Table 2 are results of this work.

The applied theoretical procedure is able to predict the surface tension of these types of mixture as a function of pressure with a very high accuracy. For this reason, it can be concluded that the extrapolation of the  $\kappa$ -value of methane to the supercritical region of methane is allowed. For the mixtures consisting of methane and hexane or of methane and heptane, only a very small difference between the results obtained with PR-EOS or PC-SAFT can be recognized. For the mixture methane + hexane, the experiments were carried out at two temperatures,  $T = 300.15$  K and  $T = 350.15$  K. The theoretical framework is able to model also the influence of temperature in excellent agreement with experimental data. For the system methane + pentane, no experimental data are available. The data given in Figure 8 are predictions for  $T = 300$  K. The predicted surface tension using PR-EOS is slightly higher than the results obtained using PC-SAFT. However, the difference between both results is always smaller than 1 mN/m.

Besides the calculation of the surface tension, the DGT permits also the calculation of the density profiles within the

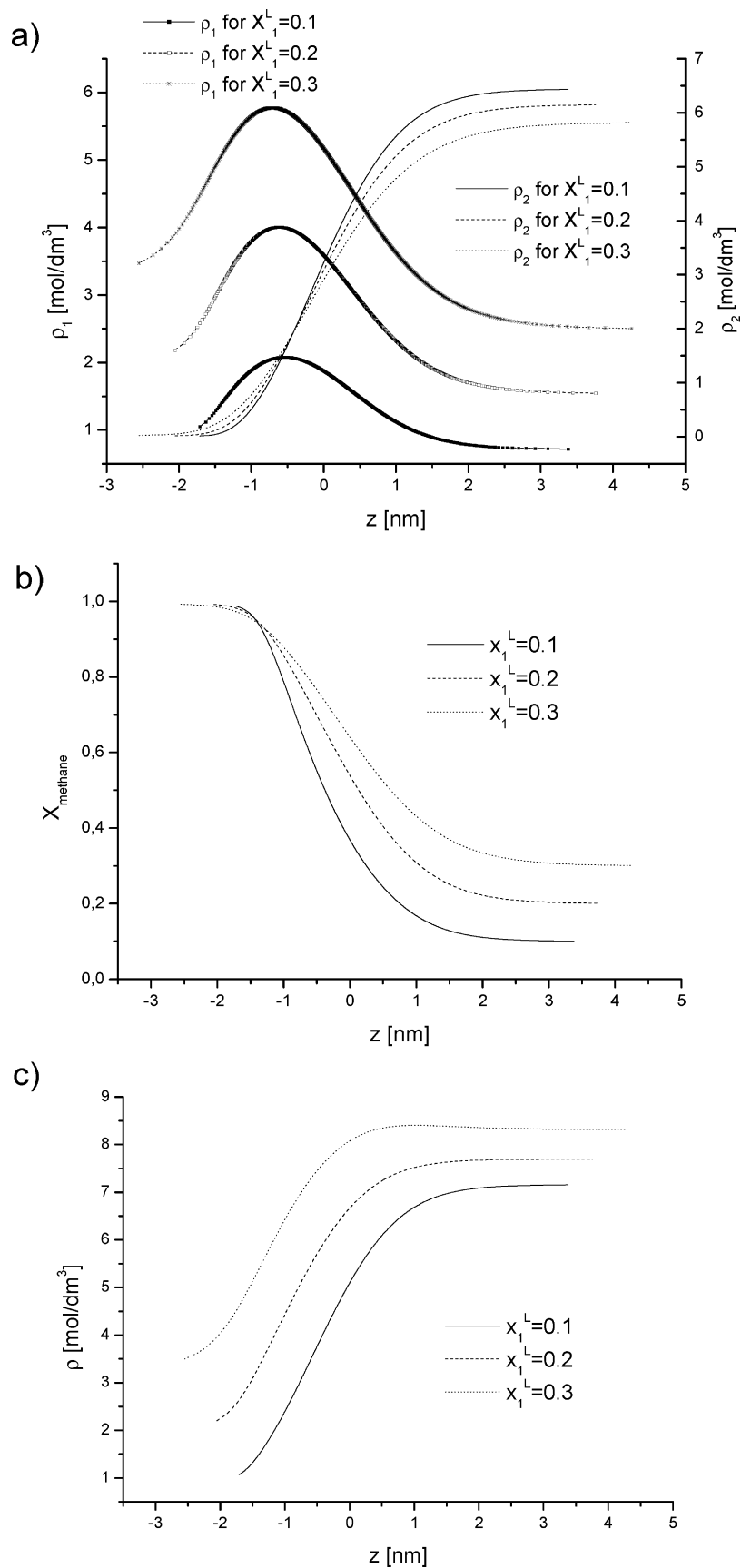


**Figure 9.** Calculated partial density (a), concentration (b), and density (c) profiles for the system methane (1) + heptane (2) using PR-EOS with  $k_{ij} = 0.03$  at 300 K and at different liquid compositions.

interface. Unfortunately, this quantity is not available by experiments. Figure 9 demonstrates the calculated partial density (a), concentration (b), and density (c) profiles for the system

methane + heptane using the PR-EOS with  $k_{ij} = 0.03$  at three different liquid compositions. The partial density profiles for heptane show the typical tanh-shape. However, the partial

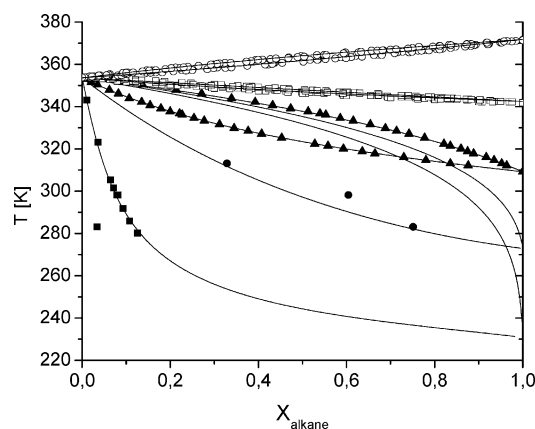


**Figure 10.** Comparison of experimental isobaric phase diagrams<sup>45</sup> and calculated phase diagrams at  $P = 0.1$  MPa for different mixtures containing cyclohexane + alkane (■ propane, ● butane, ▲ pentane, □ hexane, ○ heptane) using PR-EOS with  $k_{ij}$ -parameters given in Table 3.

**Table 3.** Estimated Binary Interaction Parameters,  $k_{ij}$ , for Binary Systems Using PR-EOS (Eq 1)

| mixture               | $k_{ij}$ |
|-----------------------|----------|
| propane + cyclohexane | 0.02     |
| butane + cyclohexane  | -0.06    |
| pentane + cyclohexane | 0        |
| hexane + cyclohexane  | -0.005   |
| heptane + cyclohexane | -0.01    |

density for the high volatile component methane runs through a maximum. This situation indicates a relative enrichment of methane in the interface leading to a resistance against the mass-transport through the interface. With increasing methane content in the liquid phase, the relative enrichment increases too. Additionally, the higher methane content in the mixture leads to a broader interface, because the density deviates at a larger distance in terms of  $z$  from the middle of the interface (at  $z = 0$ ) from the bulk value and reaches the value of the coexisting bulk phase at higher values of  $z$  if the mole fraction of methane in the liquid phase is increased. The same qualitative conclusions can be drawn by analyzing Figure 9b and c. However, the relative enrichment does not become as clear as in Figure 9a.

In summary, the PR-EOS as well as the PC-SAFT-EOS can be applied for the prediction of surface tension in mixtures.

**3. Mixtures Containing Cyclohexane +  $n$ -Alkane.** In the last chapter, it was found that both equations of state can be used for the calculation of interfacial properties. For this reason, the calculations for the systems cyclohexane +  $n$ -alkane were performed only with help of the PR-EOS. The most important condition for the calculation of interfacial properties is the accurate description of the phase behavior. To model the phase equilibrium, the binary interaction parameter  $k_{ij}$  must be obtained from experimental data. Using experimental VLE data given in the literature,<sup>47</sup> the binary interaction parameter,  $k_{ij}$ , was estimated by comparison of modeling with experimental results. The temperature-independent parameter  $k_{ij}$  was always fitted to isobaric phase equilibria data (Figure 10) and is given in Table 3. The estimated interaction parameters were tested via calculation of isothermal phase equilibria, if experimental data are available in the literature. The selected EOS works very well for the phase equilibria calculations over a broad temperature range using a temperature-independent  $k_{ij}$  value.

The experimental surface tensions were taken from the literature<sup>39</sup> and were measured with the help of the pendant-drop equipment. Using the above-discussed calculation procedure, the surface tension of the binary system can be predicted

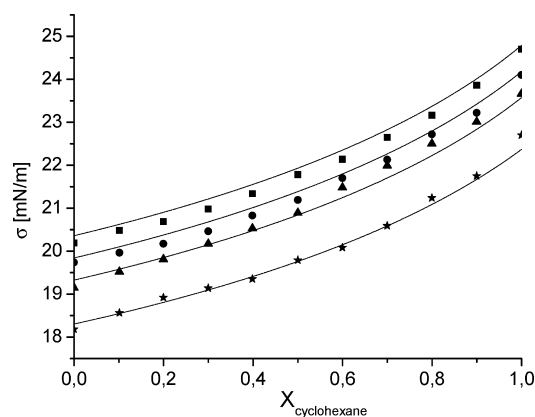


**Figure 11.** Comparison of experimental<sup>46</sup> and predicted surface tensions of the system cyclohexane + heptane at different temperatures (■  $T = 293.15$ , ●  $T = 298.15$ , ▲  $T = 303.15$ , ★  $T = 313.15$ ) using PR-EOS with  $k_{ij} = -0.01$ .

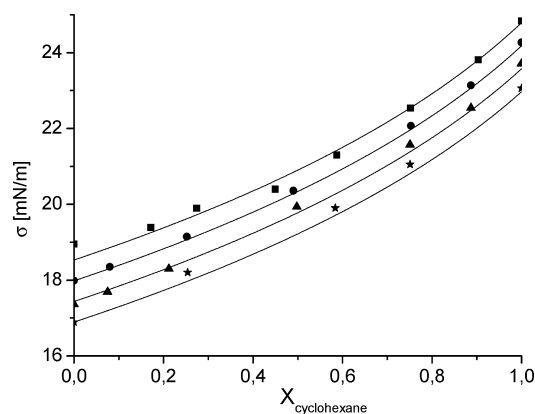


**Figure 12.** Comparison of experimental<sup>46</sup> and predicted surface tensions of the system cyclohexane + hexane at different temperatures (■  $T = 293.15$ , ●  $T = 298.15$ , ▲  $T = 303.15$ , ★  $T = 313.15$ ) using PR-EOS with  $k_{ij} = -0.005$ .

as a function of composition, temperature, and pressure. To check the quality of the suggested procedure, the predicted surface tensions were compared to experimental data<sup>46</sup> in Figure 11 for the system cyclohexane + heptane and in Figure 12 for the system cyclohexane + hexane.

The predicted surface tensions for both systems are in excellent agreement with experimental data. The suggested model is able to predict the surface tension as a function of composition and of temperature in accordance with experimental data. These findings allow us to predict the surface tension, if no experimental data are available. Figure 13 demonstrates the obtained results for the system cyclohexane + butane at different temperatures. In contrast to the systems cyclohexane + heptane or cyclohexane + hexane, the surface tension varies linearly with the cyclohexane mole fraction, where the slope is independent of temperature. For practical purposes, the following simple relationship can be used for the calculation of the surface tension for the system cyclohexane + butane as a function of temperature and mole fraction of cyclohexane in the liquid phase:

$$\sigma[\text{mN/m}] = 46.723 - 0.1167T[\text{K}] + 12.44X_{\text{cyclohexane}}^{\text{L}} \quad (15)$$

The concentration dependence of the surface tension at constant temperature for the systems cyclohexane + heptane (Figure 11) and cyclohexane + hexane (Figure 12) shows a



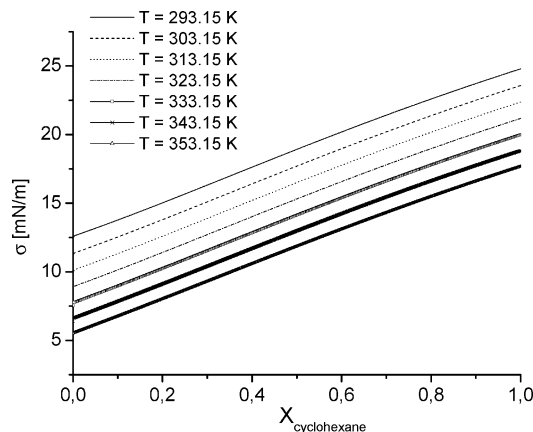


**Figure 13.** Predicted surface tensions of the system cyclohexane + butane at different temperatures using PR-EOS with  $k_{ij} = 0.06$ .

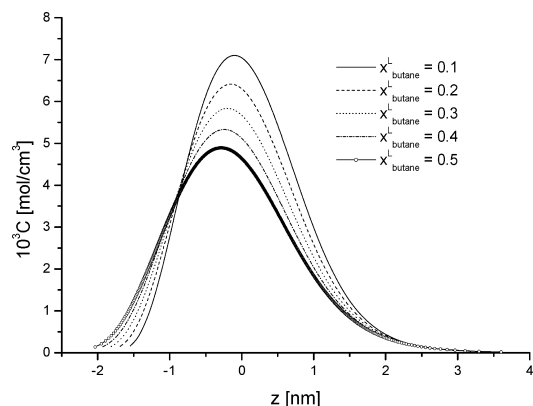


**Figure 14.** Predicted relative enrichment of butane in the interface for the system cyclohexane + butane at 298.15 K and different liquid compositions.

curved behavior. In contrast, the concentration dependence of the surface tension at constant temperature for the system cyclohexane + butane (Figure 13) shows a nearly linear behavior. One possible explanation for this result can be that the surface tensions of the pure *n*-alkanes decrease with increasing chain length at given temperature. For this reason, the difference of the surface tension of both pure components forming the mixture under consideration increases with decreasing chain length of the *n*-alkanes. Therefore, the concentration dependence changes from curved behavior to practical linear behavior. However, the last clarification can only be obtained by experiments.

The theoretical framework can be applied to calculate surface properties, which are not accessible to experimental observation, for instance, the partial density profile within the interface. The partial density profiles of butane in the system butane + cyclohexane between a liquid and a vapor phase show maxima, similar to the system methane + heptane (Figure 9). The maxima are connected with a relative enrichment of the more volatile compound. The enrichment occurs on the vapor side of the surface. The concentration dependence of the relative enrichment can be seen in Figure 14, where the *C*-function according to eq 11 is plotted for different liquid compositions. The relative enrichment decreases with the increasing butane mole fraction in the liquid phase. This phenomenon can be explained by the difference in vapor pressure.

Integration of the symmetrical interface segregation  $\Delta C(z)$  gives the relative adsorption of butane with respect to cyclohexane  $\Gamma_{AB}$  using eq 12. The results are plotted in Figure 15.

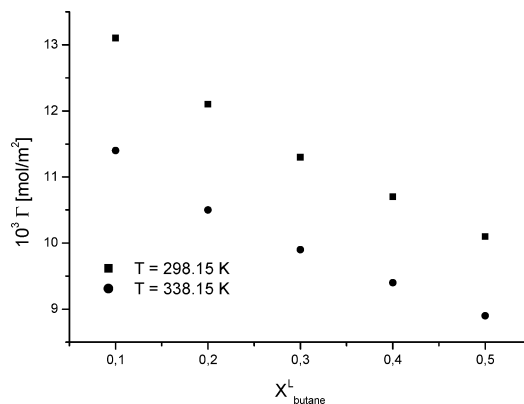


**Figure 15.** Predicted Gibbs adsorption of butane in the surface for the system cyclohexane + butane at different temperatures (■  $T = 298.15$  K, ●  $T = 338.15$  K).

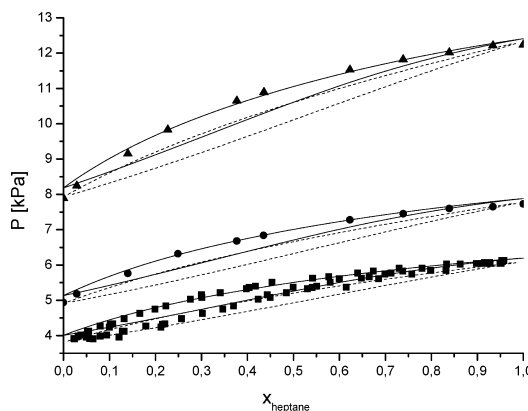


**Figure 16.** Comparison between experimental<sup>47</sup> and predicted phase behavior using PR-EOS with  $k_{ij} = 0$  (solid line) or PC-SAFT-EOS with  $k_{ij} = 0$  (broken line) for the system heptane + toluene at different temperatures (■  $T = 298.15$  K, ●  $T = 303.15$  K, ▲  $T = 313.15$  K).

The adsorption of butane in the surface decreases with increasing butane mole fraction in the liquid phase and with increasing temperatures.

In this section, the theoretical framework was used to predict surface tension values for the system cyclohexane + butane. Caused by the high vapor pressure of butane, the experiments using traditional methods, like ring method, are impossible. The theory leads to a simple relation (eq 15) allowing the calculation of surface tension as a function of temperature and liquid composition.

**4. Mixtures of *n*-Heptane + Toluene.** Kahl et al.<sup>46</sup> measured the surface tension of the system heptane + toluene at five different temperatures. The calculation of surface tensions for this system is also an excellent possibility to check the performance of the applied theory. Following our general goal to compare the performance of PR-EOS with the PC-SAFT-EOS, we apply in this section both equations in combination with DGT. The phase behavior of this system can be calculated using  $k_{ij} = 0$  for both equations, where the PR-EOS does a slightly better job for this system (Figure 16), especially at higher temperatures.

In Figure 17, the predicted surface tensions are compared to experimental data, taken from the literature,<sup>46</sup> at five different temperatures. At low temperatures ( $T = 287.81$  K), the theory predicts the surface tensions as a function of liquid composition in very good agreement with experimental values, independent of the type of equation of state. With increasing temperature,

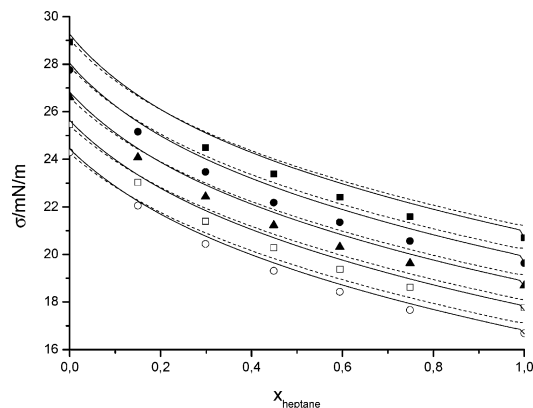


**Figure 17.** Comparison of experimental<sup>46</sup> and predicted surface tension using PR-EOS with  $k_{ij} = 0$  (solid line) or PC-SAFT-EOS with  $k_{ij} = 0$  (broken line) for the system heptane + toluene at different temperatures (■  $T = 287.81$  K, ●  $T = 297.15$  K, ▲  $T = 307.86$  K, □  $T = 317.86$  K, ○  $T = 327.86$  K).

the difference between the theoretical and experimental surface tensions increases; however, all deviations are smaller than 0.5 mN/m.

## Conclusions

As a conclusion, it can be said that the DGT in combination with a suitable equation of state (PR-EOS or PC-SAFT) is a powerful tool for the prediction of surface tensions of binary mixtures. In the case of PR-EOS, only experimental data of the critical pressure, the critical temperature, the acentric factor, and one surface tension at one temperature for the pure components and one binary interaction parameter adjusted to bulk phase equilibria are necessary to predict the surface tension. In the case of PC-SAFT-EOS, additional vapor pressures and liquid volumes of the pure components must be known caused by the different parameter fitting procedure of the pure-component parameters.

For the type of mixtures studied in this Article, no significant difference between both equations of state could be found. Both equations in combination with the DGT accurately predict phase behavior and surface tensions of mixtures consisting of nonpolar molecules over a wide range of temperatures and pressures. However, if polar molecules are present in the mixture, the PC-SAFT-EOS should be applied rather than the PR-EOS. The theoretical framework was applied to predict the surface tension of mixtures also in the case if no experimental data are available.

## Acknowledgment

We thank Twister B.V. (Netherlands) for fruitful discussion and financial support.

## Appendix

### List of Symbols

$f$  = Helmholtz free energy density  
 $k$  = Boltzmann constant  
 $p$  = pressure  
 $R$  = gas constant  
 $T$  = temperature  
 $v$  = volume  
 $z$  = distance perpendicular to the surface

### Greek Symbols

$\kappa$  = influence parameter  
 $\rho$  = density  
 $\sigma$  = surface tension

### Subscripts

0 = homogeneous state  
 c = critical state

### Superscripts

ideal = ideal gas term  
 L = liquid phase  
 V = vapor phase

## Literature Cited

- (1) Cahn, J. W.; Hilliard, J. E. Free energy of a nonuniform system. I. Interfacial free energy. *J. Chem. Phys.* **1958**, *28*, 258–267.
- (2) Poser, C. I.; Sanchez, I. C. Interfacial tension theory of low and high molecular weight liquid mixtures. *Macromolecules* **1981**, *14*, 361–70.
- (3) Cornelisse, P. M. W. The gradient theory applied. Simultaneous modelling of interfacial tension and phase behaviour. Thesis, TU Delft, 1997.
- (4) Enders, S.; Quitzsch, K. Calculation of interfacial properties of demixed fluids using density gradient theory. *Langmuir* **1998**, *14*, 4606–4614.
- (5) Zuo, Y. X.; Stenby, E. H. Calculation of interfacial tensions with gradient theory. *Fluid Phase Equilib.* **1997**, *132*, 139–158.
- (6) Miqueu, C.; Mendiboure, B.; Graciaa, A.; Lachaise, J. Modeling of the surface tension of multicomponent mixtures with the gradient theory of fluid interfaces. *Ind. Eng. Chem. Res.* **2005**, *44*, 3321–9.
- (7) Müller, E. A.; Gubbins, K. E. Molecular-based equation of state for associating fluids: A review of SAFT and related approaches. *Ind. Eng. Chem. Res.* **2001**, *40*, 2193–2211.
- (8) Ting, P. D.; Joyce, P. C.; Jog, P. K.; Chapman, W. G.; Thies, M. C. Phase equilibrium modeling of mixtures of long-chain and short-chain alkanes using Peng-Robinson and SAFT. *Fluid Phase Equilib.* **2003**, *206*, 267–86.
- (9) Ghosha, A.; Chapman, W. G.; French, R. N. Gas solubility in hydrocarbons - a SAFT-based approach. *Fluid Phase Equilib.* **2003**, *209*, 229–43.
- (10) Benzaghrou, S.; Passarello, J. P.; Tobaly, P. Predictive use of a SAFT EOS for phase equilibria of some hydrocarbons and their binary mixtures. *Fluid Phase Equilib.* **2001**, *180*, 1–26.
- (11) Economou, I. C. Statistical associating fluid theory: A successful model for the calculation of thermodynamic and phase equilibrium properties of complex fluid mixtures. *Ind. Eng. Chem. Res.* **2002**, *41*, 953–62.
- (12) dos Ramos, M. C.; Blas, J. F.; Galindo, A. Modeling the phase equilibria and excess properties of the water + carbon dioxide binary mixture. *Fluid Phase Equilib.* **2007**, *261*, 359–365.
- (13) Kahl, H.; Enders, S. Calculation of surface properties of pure fluids using density gradient theory and SAFT-EOS. *Fluid Phase Equilib.* **2000**, *172*, 27–42.
- (14) Enders, S.; Kahl, H. Interfacial properties of binary mixtures. *Phys. Chem. Chem. Phys.* **2002**, *4*, 931–936.
- (15) Enders, S.; Kahl, H. Interfacial properties of water + alcohol mixtures. *Fluid Phase Equilib.* **2008**, *263*, 160–167.
- (16) Gross, J.; Sadowski, G. Perturbed-chain SAFT: An equation of state based on a perturbation theory for chain molecules. *Ind. Eng. Chem. Res.* **2001**, *40*, 1244–1260.
- (17) Gross, J.; Sadowski, G. Modeling polymer systems using the perturbed-chain statistical associating fluid theory equation of state. *Ind. Eng. Chem. Res.* **2002**, *41*, 1084–93.
- (18) Chapman, W. G.; Sauer, S. G.; Ting, D.; Ghosh, A. Phase behavior applications of SAFT based equations of state from associating fluids to polydisperse, polar copolymers. *Fluid Phase Equilib.* **2004**, *217*, 137–43.
- (19) Jog, P. K.; Sauer, S. G.; Blaesing, J.; Chapman, W. G. Application of dipolar chain theory to the phase behavior of polar fluids and mixtures. *Ind. Eng. Chem. Res.* **2001**, *40*, 4641–8.
- (20) Dominik, A.; Chapman, W. G.; Kleiner, M.; Sadowski, G. Modeling of polar systems with the perturbed-chain SAFT equation of state. Investigation of the performance of two polar terms. *Ind. Eng. Chem. Res.* **2005**, *44*, 6928–38.
- (21) Barker, J. A.; Henderson, D. Perturbation theory and equation of state for fluids: The square-well potential. *J. Chem. Phys.* **1967**, *47*, 2856–61, 4714–21.

- (22) Sarman, S.; Greberg, H.; Satherley, J.; Penfold, R.; Nordholm, S. Effective potential approach to bulk thermodynamic properties and surface tension of molecular fluids II. Binary mixture of *n*-alkanes and miscible gas. *Fluid Phase Equilib.* **2000**, *172*, 145–167.
- (23) Panayiotou, C. Interfacial tension and interfacial profiles of fluids and their mixture. *Langmuir* **2002**, *18*, 8841–53.
- (24) Kiselev, S. B.; Ely, J. F. Generalized corresponding state model for bulk and interfacial properties in pure fluids and fluid mixtures. *J. Chem. Phys.* **2003**, *119*, 8645–62.
- (25) Miqueu, C.; Mendiboure, B.; Gracia, C.; Lachaise, J. Generalized corresponding state model for bulk and interfacial properties in pure fluids and fluid mixtures. *Fluid Phase Equilib.* **2004**, *218*, 189–203.
- (26) Miqueu, C.; Mendiboure, B.; Gracia, A.; Lachaise, J. Modeling of the surface tension of multicomponent mixtures with the gradient theory of fluid interfaces. *Ind. Eng. Chem. Res.* **2005**, *44*, 3321–9.
- (27) Gloor, G. J.; Jackson, G.; Blas, F. J.; del Ro, E. M.; Miguel, E. Prediction of the vapor–liquid interfacial tension of nonassociating and associating fluids with the SAFT-VR density functional theory. *J. Phys. Chem. C* **2007**, *111*, 15513–22.
- (28) Dominik, A.; Tripathi, S.; Chapman, W. G. Bulk and interfacial properties of polymers from interfacial SAFT density functional theory. *Ind. Eng. Chem. Res.* **2006**, *45*, 6785–6792.
- (29) Wu, J. Density functional theory for chemical engineering: From capillarity to soft materials. *AIChE J.* **2006**, *52*, 1169–1193.
- (30) Andreas, J. M.; Hauser, E. A.; Tucker, W. B. Boundary tension by pendant drop. *J. Phys. Chem.* **1938**, *42*, 1001–1019.
- (31) Davis, H. T. *Statistical Mechanics of Phases, Interfaces, and Thin Films*; Wiley-VCH: New York, Chichester, Weinheim, Brisbane, Singapore, Toronto, 1996.
- (32) Jaeger, P.; Pietsch, A. Characterization of reservoir systems at elevated pressure. *J. Petrol. Sci. Eng.* **2009**, *64*, 20–24.
- (33) Krüss: Drop Shape Analysis. Benutzerhandbuch. Krüss GmbH, Hamburg, 1997.
- (34) Jaeger, P.; Eggers, R.; Baumgartl, H. Interfacial properties of high viscous liquids in a supercritical carbon dioxide atmosphere. *J. Supercrit. Fluids* **2002**, *24*, 203–217.
- (35) Jaeger, P.; Eggers, R. Interfacial tension of ionic liquids at elevated pressures. *Chem. Eng. Proc.* **2009**, *48*, 1173–1176.
- (36) Jaeger, P.; Eggers, R. Liquid–liquid interphase at high pressures in presence of compressible fluids. *Thermochim. Acta* **2005**, *438*, 16–21.
- (37) NIST data tables.
- (38) Peng, D. Y.; Robinson, D. B. A new two-constant equation of state. *Ind. Eng. Chem. Fundam.* **1976**, *15*, 59–64.
- (39) Wohlfarth, Ch.; Wohlfarth, B. In *Numerical Data and Functional Relationships in Science and Technology, Vol. 16: Surface Tension of Pure Liquids and Binary Liquid Mixtures*; Lechner, M. D., Ed.; Landoldt-Börnstein, New Series Group IV Physical Chemistry; Springer Verlag: Berlin, Heidelberg, 1997.
- (40) Telo da Gama, M. M.; Evans, R. The structure and surface tension of the liquid-vapor interface near the upper critical end point of a binary mixture of Lennard-Jones fluids. *Mol. Phys.* **1983**, *48*, 229–250.
- (41) Wadewitz, T.; Winkelmann, J. Density functional theory: Structure and interfacial properties of binary mixtures. *Ber. Bunsen-Ges. Phys. Chem.* **1996**, *100*, 1825–33.
- (42) Lekner, J.; Henderson, J. Theoretical determination of the thickness of a liquid–vapour interface. *Physica A* **1978**, *94*, 545–558.
- (43) Reamer, H. H.; Sage, B. H.; Lacey, W. N. Volumetric and phase behavior of the methane-*n*-heptane system. *Chem. Ing. Data Ser.* **1956**, *1*, 29–42.
- (44) Bett, K. E.; Juren, B.; Reynolds, R. G. Phase equilibria in methane/*n*-alkane binary mixtures under pressure. Physical properties of liquid and gases for plant and process design. *Edinburgh* **1970**, 53–67.
- (45) Busch, A.; Grau, G. G.; Kast, W.; Klemm, A.; Kohl, W.; Kux, C.; Meyerhoff, G.; Neckel, A.; Ruhtz, E.; Schäfer, K.; Valentiner, S. In *Eigenschaften der Materie in ihren Aggregatzuständen 2. Teil, Gleichgewichte Dampf-Kondensat und osmotische Phänomene*; Schäfer, K., Lax, E., Eds.; Landoldt Börnstein IV; Springer Verlag: Berlin, Göttingen, Heidelberg, 1960.
- (46) Kahl, H.; Wadewitz, T.; Winkelmann, J. Surface tension and interfacial tension of binary organic liquid mixtures. *J. Chem. Eng. Data* **2003**, *48*, 1500–7.
- (47) Soerensen, J. M.; Arlt, W. *Vapour–Liquid Equilibrium Data Collection, Bd 1, Binary Systems*; DECHEMA Frankfurt/Main, 1979.

Received for review July 30, 2009

Revised manuscript received October 14, 2009

Accepted November 16, 2009

IE901209Z